Precision Engineering 57 (2019) 244–252

Contents lists available at ScienceDirect

Precision Engineering

journal homepage: www.elsevier.com/locate/precision

Formation behavior of laser-induced periodic surface structures on stainless tool steel in various media

Tomoki Kobayashi[a], Tomohiro Wakabayashi[b], Yuichi Takushima[c], Jiwang Yan[a,*]

[a] Department of Mechanical Engineering, Keio University, Hiyoshi 3-14-1 Kohoku, Yokohama, Kanagawa, 223-8522, Japan
[b] Yazaki Corporation, Hikarinooka 3-1, Yokosuka, Kanagawa, 239-0847, Japan
[c] Optoquest Co.Ltd, Haraiti 1335 Ageo, Saitama, 362-0021, Japan

ARTICLE INFO

Keywords:
Laser-induced periodic surface structure
Nanostructure
Picosecond pulsed laser
Refractive index
Surface topography

ABSTRACT

The formation of laser-induced periodic surface structure (LIPSS) has been observed on various materials. As LIPSS can be used for modifying various surface properties such as wettability, tribology and optical performance, the control of the period and topography of LIPSS is an important issue. In this study, picosecond pulsed laser irradiation was performed on a stainless tool steel in various types of media including the air, water, sugar syrup (water and sucrose ($C_{12}H_{22}O_{11}$)), decane ($C_{10}H_{22}$), and ethanol (C_2H_5OH). Different surface morphologies were observed on the steel surface after laser irradiation, depending on the types of media. A strong relationship was identified between the period of LIPSS and the refractive index of liquid. In addition to the change of LIPSS period, complicated mesh patterns were formed on the surface irradiated in decane and ethanol, indicating the significant effect of thermal conductivity of the liquids on surface formation mechanisms. This study demonstrated the possibility of controlling the period and topography of LIPSS by using different media.

1. Introduction

Laser-induced periodic surface structures (LIPSS) have been obtained on various materials such as metals, semiconductors, and dielectrics [1–4]. LIPSS is formed when an ultrashort pulsed laser is irradiated near the ablation threshold of a material [5,6]. It is well known that normally the period of LIPSS induced by an ultrashort pulse laser is slightly shorter than the wavelength of the laser [7]. The shape and orientation of LIPSS are influenced by the polarization of the laser [8–10]. However, there is still considerable ambiguity about the mechanism of LIPSS formation. One of the possible mechanisms is the interference of the laser beam and a laser-excited electric field called surface plasmon polariton (SPP) [11,12]. An electrical charge distribution is immediately generated on the surface by laser irradiation, and this electrical charge distribution induces SPP. LIPSS is a result of ablation on the modulated energy deposition caused by the interference of the incident laser and the SPP. Another proposed mechanism for LIPSS formation is the laser-induced self-organization of materials [5,13]. The emission of electrons caused by laser absorption induces instability of the surface, and the lattice is perturbed. As a result, LIPSS is assembled by surface relaxation due to the instability of the surface. It is generally accepted that the dominant LIPSS formation mechanism depends on the property of the workpiece material used.

As LIPSS can be utilized to generate various surface properties such as wettability [14–16], tribological [17] and optical performances [18,19], the control of the period and topography of LIPSS is a critical issue. It has been found that the period and topography of LIPSS are related to various laser parameters such as wavelength [7,20], fluence [11], number of pulses [21–23], incident angle [24,25] and polarization [8]. However, up to date, few studies have focused on controlling the morphology of LIPSS by changing the surrounding media. Although it was reported that the period of LIPSS formed in a liquid was shorter than that in the air, the relationship between the morphology of LIPSS and the medium properties is still unclear [26].

In this study, the authors attempted forming LIPSS with various periods on a steel surface by irradiating a picosecond pulsed laser in different types of surrounding media. The aim is to control the morphology of LIPSS by utilizing the difference in the refractive index and thermal conductivity of various types of media. The control of the period of LIPSS is useful for enhancing the surface properties such as hydrophobicity and friction reduction. LIPSS on a steel mold can improve the mold releasing ability in plastic molding applications [4]. In addition to the improvement in these surface properties, LIPSS can also be used as diffraction gratings to generate structural colors [19]. Laser processing of workpiece in liquids can prevent from surface oxidation, impurity contamination and particle adhesion, as well as thermal deformation of the workpiece.

* Corresponding author.
E-mail address: yan@mech.keio.ac.jp (J. Yan).

https://doi.org/10.1016/j.precisioneng.2019.04.012
Received 22 November 2018; Received in revised form 2 April 2019; Accepted 16 April 2019
Available online 30 April 2019

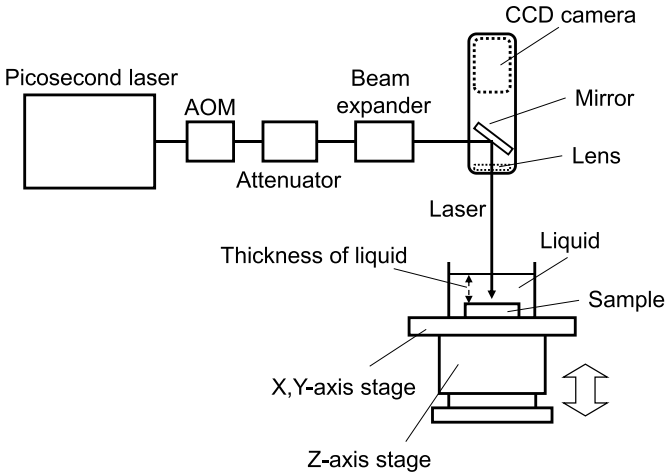

Fig. 1. Schematic of the experimental setup.

Table 1
Properties of liquids used.

	Density [g/cm^3]	Refractive index	Thermal conductivity [W/m K]
Water	0.997	1.33	0.609 (27 °C)
Sugar syrup (60%)	1.29	1.44	–
Decane	0.730	1.41	0.147 (27 °C)
Ethanol	0.789	1.36	0.163 (30 °C)

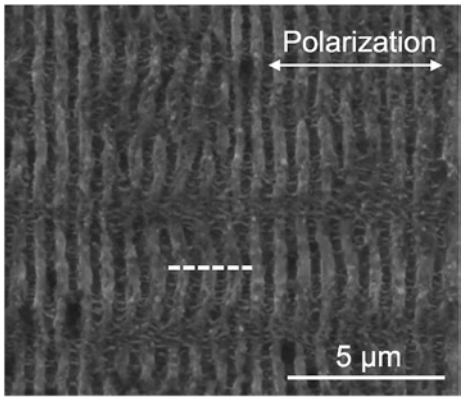

Fig. 2. SEM image of LIPSS formed in the air.

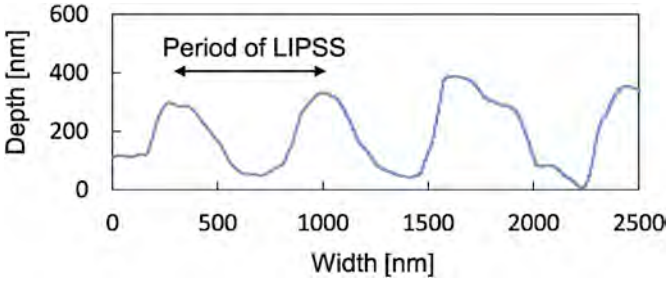

Fig. 3. Cross-sectional profile of LIPSS showing period measurement method.

2. Experimental method

The laser used in the experiments was an Yb fiber laser, PFLA-1030TP, produced by Optoquest Co., Ltd. The wavelength was 1030 nm and the pulse width was 50 ps The energy density of the laser beam had a Gaussian distribution. Fluence was changed between 0.15 and 0.76 J/cm^2, and the repetition frequency was set to 10 and 100 kHz. The laser beam was focused into an elliptical spot with a size of 6 μm × 7 μm, and the focal length was 20 mm. A stage was used to move the workpiece in the X-, Y- and Z-axis directions. The focal point of the laser beam was adjusted by a lens, and a CCD camera was used to observe the laser spot on the workpiece surface, as shown in Fig. 1. The laser scan speed was set to 1 and 40 mm/s, and the overlap between two neighboring scan lines was 2 μm. A stainless steel consisting of C (0.38%), Si (0.9%), Mn (0.5%), Cr (13.6%), V (0.3%) was used as workpiece. The sample size was 20 mm × 20 mm × 5 mm.

Refractive index and thermal conductivity are considered to be the most important properties of a medium for laser irradiation: the former affects the laser incident angle and focusing distance, while the latter influences the heat absorption at the irradiated surface. To investigate the effects of these factors on LIPSS formation, in this study, the workpiece was irradiated in 4 kinds of media, namely the air, water, sugar syrup (water and sucrose ($C_{12}H_{22}O_{11}$)), decane ($C_{10}H_{22}$) and ethanol (C_2H_5OH), respectively. The concentration of sugar syrup was 60%. The refractive index and thermal conductivity of all these liquids are different. The properties of the liquids are shown in Table 1. The thickness of the liquid layer over the workpiece was changed within 3–9 mm.

The obtained surface structure was observed by a scanning electron microscope (SEM), INSPECT S50 produced by FEI Company. The profile of the surface structure was measured by an atomic force microscope (AFM), SPM-3 produced by Hitachi High-Technologies Corporation.

3. Results and discussion

3.1. LIPSS formation in the air

The laser was irradiated in the air with a fluence of 0.15 J/cm^2 at a repetition frequency of 100 kHz and a scanning speed of 40 mm/s. The SEM image of the irradiated surface is shown in Fig. 2. The arrow in the image shows the direction of laser polarization. LIPSS perpendicular to the laser polarization was formed on the surface. The cross-sectional profile of the LIPSS is shown in Fig. 3. The profile was plotted along the dotted line in Fig. 2. The period of LIPSS was defined as the average distance between the peaks of the LIPSS which can be measured from the cross-sectional profile. The period of LIPSS was 726 nm, shorter than the laser wavelength (1030 nm). This kind of LIPSS was defined as low spatial frequency LIPSS (LSFL), the period of which is slightly shorter than the laser wavelength [27].

3.2. Effect of refractive index of media

In order to investigate the effect of the refractive index of liquids, the laser was irradiated in water and sugar syrup with a fluence of 0.76 J/cm^2 at a frequency of 10 kHz and a scanning speed of 1 mm/s. A higher fluence was used than in the air because liquids absorb laser more than the air. If the scanning speed of the stage is too fast, the water surface will surge and cause the defocus of laser. To prevent

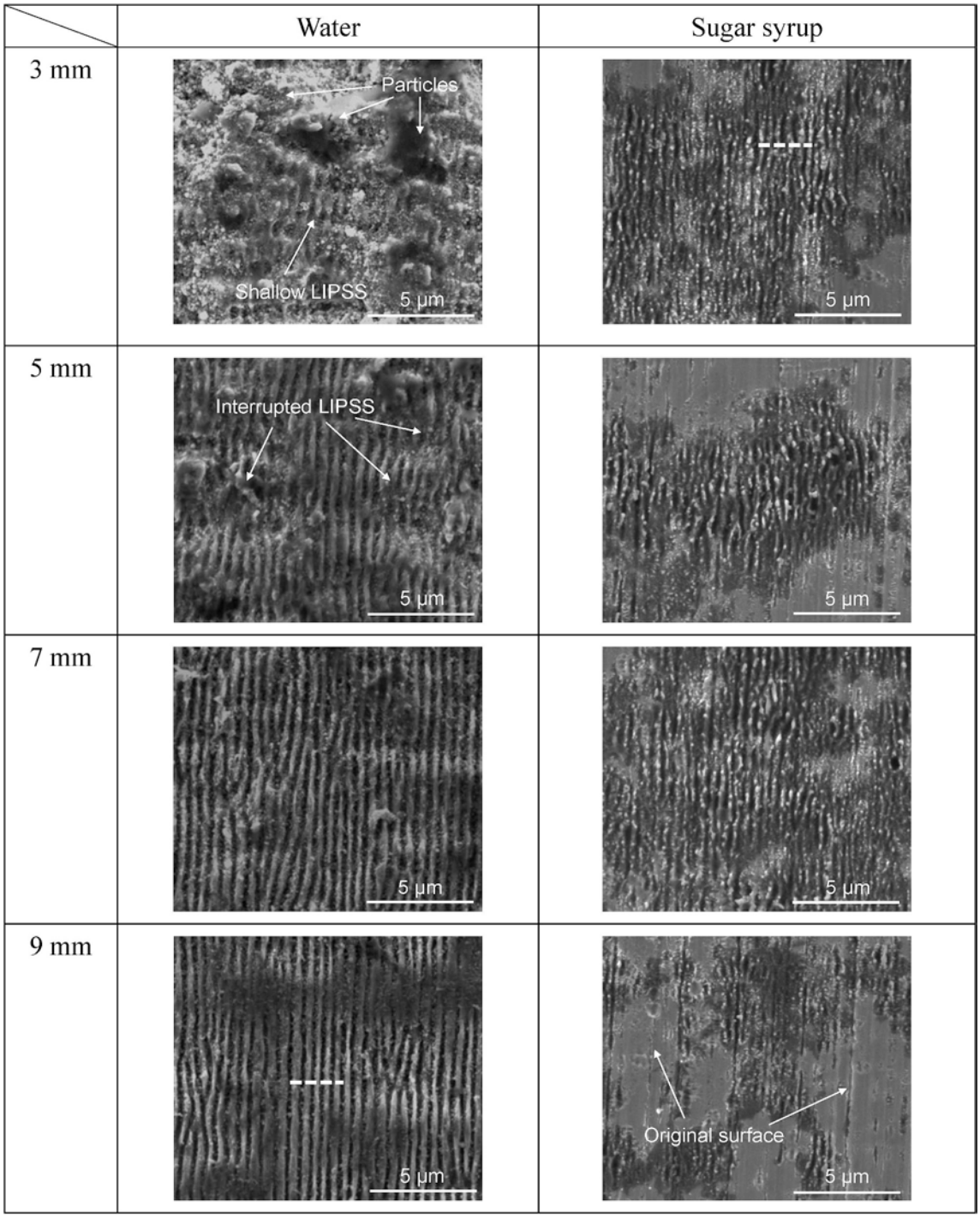

Fig. 4. SEM images of surfaces irradiated in water and sugar syrup at various thicknesses of liquid layer.

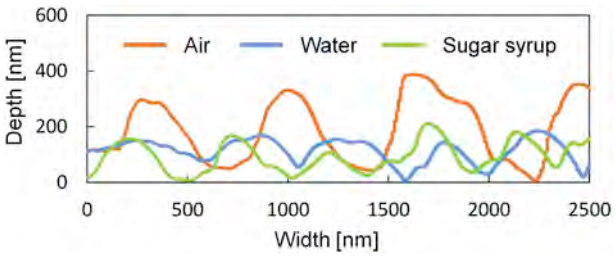

Fig. 5. Cross-sectional profiles of LIPSS formed in the air, water and sugar syrup.

water surging, a slow scanning speed was used. Accordingly, the frequency of laser pulse was also decreased.

The SEM images of the surface irradiated in water and sugar syrup at different liquid thicknesses are shown in Fig. 4. When the laser was irradiated in water, the surface morphology was changed depending on the thickness of water layer. When the water layer was 3 mm thick, very shallow LIPSS was observed only on a few areas of the surface; the surface was roughened and covered with many particles. At 5 mm thickness of water, LIPSS was formed but partially interrupted. When the thickness of water was over 7 mm, LIPSS was regularly formed on the entire surface. This change of surface structures might be due to the difference in laser absorption amount by water. If the water layer is

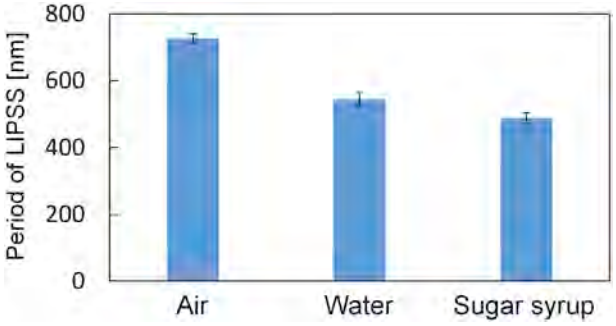

Fig. 6. Periods of LIPSS formed in the air, water and sugar syrup.

Table 2
Experimental and calculation result of the period of LIPSS formed in liquids.

	Water	Sugar syrup
Experiment	526 nm	482 nm
Calculation	546 nm	504 nm

thin, the laser absorption is small, and the laser fluence remains high when reaching the surface. Thus, thermal effect occurs and causes material melting [28]. On the other hand, if the water layer becomes thicker, the laser fluence decreases to be near the ablation threshold, thus LIPSS is formed on the surface.

When the laser was irradiated in sugar syrup, fine LIPSS was formed on the surface at each liquid thickness from 3 to 7 mm. However, when the sugar syrup layer was further thicker (9 mm), LIPSS becomes very shallow and formed partially on the surface while unaffected surface regions remained. This indicates that the laser absorption in sugar syrup is more significant than that in water, and laser fluence is too low to induce LIPSS due to the excessive laser absorption by the thick sugar syrup layer.

Another noteworthy phenomenon was that laser-induced bubble generation was more significant in sugar syrup than in water. Laser-induced plasma in liquid changes into bubbles after cooling [29], which block the subsequent laser pulses and make the irradiation process unstable. As a result, the LIPSS generation becomes non-uniform and the surface area with LIPSS formation is decreased. It is known that sugar syrup has a higher viscosity than water, thus is easier to induce bubbles [30]. In Fig. 4, surface regions without LIPSS formation can be clearly identified for laser irradiation in sugar syrup. At liquid layer thicknesses of 5 and 9 mm, the unaffected surface areas were especially bigger, indicating more significant bubble formation and process instability.

The cross-sectional profiles of the LIPSS formed in water (thickness: 9 mm) and sugar syrup (thickness: 3 mm) are shown in Fig. 5. The profiles were plotted along the dotted lines in Fig. 4. To compare the period of LIPSS, the cross-sectional profile of LIPSS formed in the air (Fig. 3) is replotted in Fig. 5. In Fig. 5, it can be seen that the period of LIPSS formed in a liquid is shorter than that in the air. The average period of LIPSS for each medium was shown in Fig. 6. The period was 726 nm in the air, while decreased to 526 nm in water, and 482 nm in sugar syrup. From Fig. 5, it can be seen that not only the LIPSS period, but also the LIPSS height was decreased for laser irradiation in liquids compared to laser irradiation in the air.

It is assumable that the refractive index of the liquids caused the changes of the period of LIPSS. When the light passes through the boundary of media with different refractive index, the wavelength of light is changed according to the Snell's equation:

$$n_1 \cdot \lambda_1 = n_2 \cdot \lambda_2 \quad (1)$$

where n_1 is the refractive index of material 1, λ_1 the wavelength of light in material 1, n_2 the refractive index of material 2, and λ_2 the wavelength of light in material 2. When the laser travels from the air to a liquid, the wavelength of laser becomes shorter because of the change in the refractive index. As a result, the period of LIPSS formed in the liquid becomes shorter because the LIPSS period is related to the wavelength of laser [7]. Then, the period of LIPSS formed in a liquid can be calculated by the following equation:

$$\delta_1 = \delta_a / n_1 \quad (2)$$

where δ_l is the period of LIPSS formed in the liquid, δ_a the period of LIPSS formed in the air, and n_l the refractive index of the liquid. The calculated and experimental results of the period of LIPSS formed in liquids are shown in Table 2. The experimental result and the calculation result are very close, which strongly demonstrates the relationship between the period of LIPSS and the refractive index of a liquid.

3.3. Effect of thermal conductivity of media

In order to investigate the effect of thermal conductivity of a liquid, the laser was irradiated in decane and ethanol with an fluence of 0.76 J/cm^2 at a pulse frequency of 10 kHz, and a scan speed of 1 mm/s. The SEM images of the surface irradiated at different thicknesses of liquid layer are shown in Fig. 7. Unlike in water, complicated patterns were formed in decane and ethanol. When the layer of liquids was thin (~5 mm), a mesh structure was formed on the entire surface. However, when the liquid layer thickness was over 7 mm, a periodic straight nanoscale grooves were formed on the surface in addition to the mesh patterns.

Mesh structures have been reported in previous research of laser irradiation on metal surfaces, where thermal effect due to high laser fluence is dominant [31]. In this research, the mesh structures might have been formed by the heat of plasma generated inside the liquid. The spread of laser-induced plasma is suppressed by the surrounding liquid; thus the high-temperature plasma is kept near the surface for a long time [32]. The suppressed plasma generates a strong thermal effect on the irradiated surface, leading to formation of mesh structures, as schematically shown in Fig. 8. In this process, the thermal conductivity of the liquid might take an important role on surface morphology formation. As shown in Table 1, the thermal conductivity of decane and ethanol was distinctly lower than that of water. The low thermal conductivity prevents the heat of plasma from escaping to the surrounding media. As a result, the thermal effect becomes stronger and mesh structure is formed.

3.4. Effect of media on LIPSS reassembly

In the previous sections, we have examined the LIPSS formation on a flat surface and confirmed the period and morphology changes of the LIPSS depending on the media. Then we have the question: what will happen if laser irradiation is performed on a surface with existing LIPSS? In the following experiment, the laser was irradiated on the surface where LIPSS was already formed. In other words, two-step irradiation was performed in different combinations of media; the effect of media type on LIPSS reassembly in the second irradiation were investigated. In this paper, results for two-step irradiation in 3 media

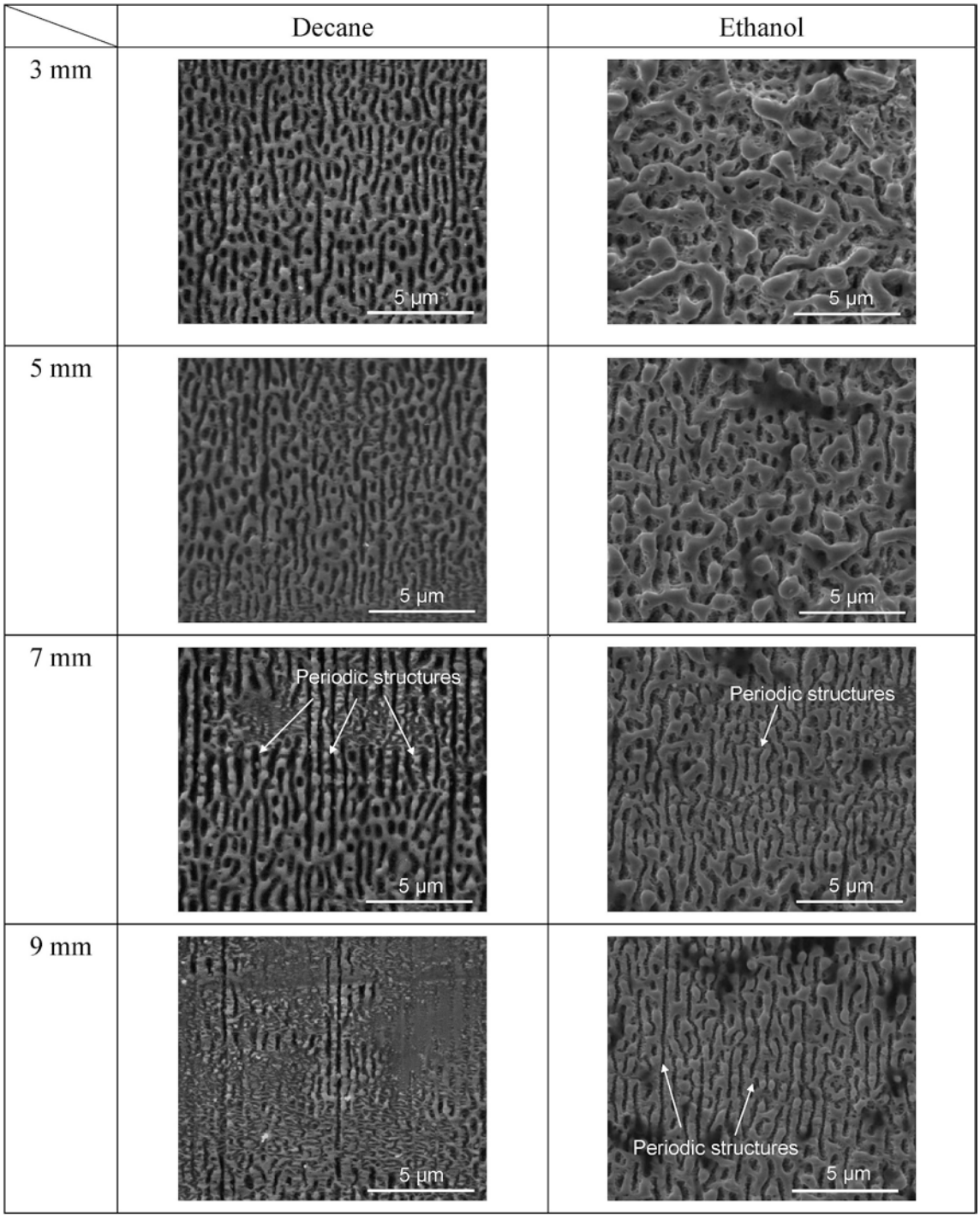

Fig. 7. SEM images of surfaces irradiated in decane and ethanol at various thicknesses of liquid layer.

combinations (air-air, water-air, and air-water) are presented. The laser irradiation conditions are: laser fluence 0.15 J/cm^2, pulse frequency 100 kHz, and laser scan speed 40 mm/s in the air; laser fluence 0.76 J/cm^2, pulse frequency 10 kHz, and laser scan speed 1 mm/s in water (thickness: 9 mm).

First, the laser was irradiated in the air on a flat surface, and then irradiated again in the air on the same area. The SEM images of the irradiated surface are shown in Fig. 9. LIPSS was formed on the surface by the first irradiation (Fig. 9 (a)). After the second irradiation, LIPSS with the same period was formed (Fig. 9 (b)). LIPSS was continuously formed even at the boundary without period difference and phase shift of LIPSS observed (Fig. 9 (c), (d)).

Next, the laser was irradiated in water on a flat surface and then irradiated in the air on the same area. The SEM images of the irradiated

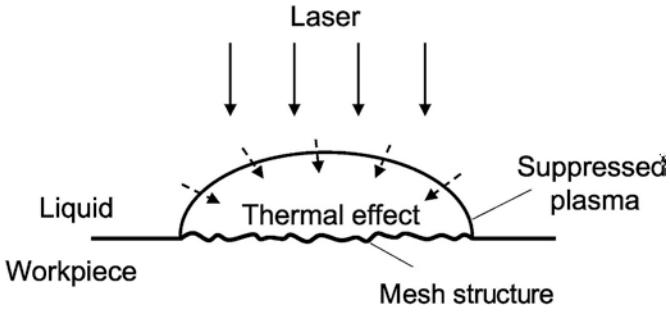

Fig. 8. Thermal effect caused by suppressed plasma expansion inside a liquid.

surface are shown in Fig. 10. LIPSS with a shorter period than that in Fig. 9 (a) was formed by first irradiation in water (Fig. 10 (a)). After the second irradiation in the air, similar LIPSS remained on the surface (Fig. 10 (b)). At the boundary of (a) and (b), LIPSS was continuously formed without phase shift or period change (Fig. 10 (c), (d)).

Fig. 11 shows the cross-sectional profiles of LIPSS shown in Figs. 9 (b) and 10 (b) plotted along the dotted lines. Although both the two kinds of LIPSS were finally formed in the air, the period of LIPSS formed in air after water was shorter than that formed in air after air. This result indicated that the period of LIPSS formed in the air was dependent on the period of the former LIPSS.

As the next experiment, the laser was irradiated in the air on a flat surface and then irradiated in water on the same area. The SEM images of the irradiated surface are shown in Fig. 12. Compared to the LIPSS formed in the first irradiation in air (Fig. 12 (a)), the LIPSS formed by the second irradiation in water has a distinctly shorter period (Fig. 12 (b)). Due to the period difference, there is an apparent phase mismatch at the boundary (Fig. 12 (c)), where LIPSS was bifurcated after the second irradiation (Fig. 12 (d)). This result showed that the period of LIPSS formed in water was independent of that generated in the first laser irradiation.

3.5. Effect of media on LIPSS reassembling mechanism

Based on the experimental results in the previous sections and the findings from previous studies, the mechanism of LIPSS formation are discussed as follows. In general, two mechanisms of LIPSS formation are possible in laser irradiation on metals, as shown in Fig. 13. One is based on the interference of laser and SPP (Fig. 13 (a)), and the other is based on the self-organization of material surface (Fig. 13 (b)).

As shown in Fig. 13 (a), the initial stage of LIPSS formation is caused by the ablation on the modulated energy deposition due to the interference of incident laser and SPP [11,12]. Then, the electric field is modulated along the initially formed structures. As a result, the electric field is strengthened inside the grooves to make them deeper. As the number of pulses increases, the groove depth is further amplified through the ablation effect and LIPSS is finally formed on the surface. In this case, LIPSS formation depends strongly on the initial surface structure [11]. If there are existing grooves before irradiation, the electric field will be strengthened inside those grooves to make them deeper without changing their period.

On the other hand, LIPSS formation can be induced by surface

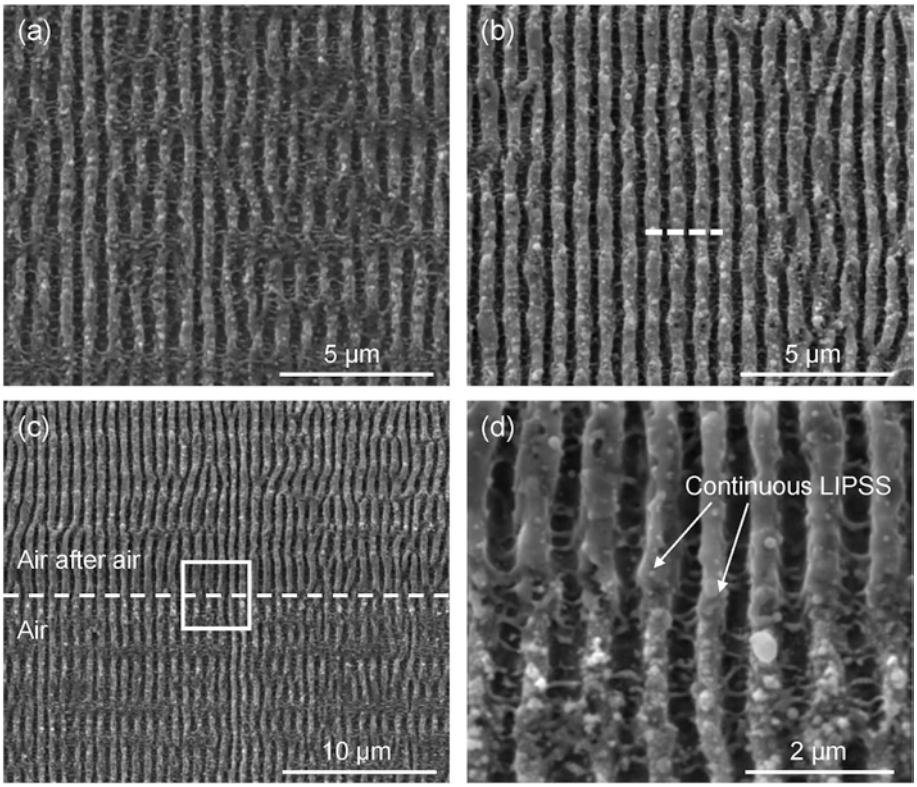

Fig. 9. SEM images of the surface (a) after the first irradiation and (b) after the second irradiation in the air; (c) boundary region of (a) and (b); (d) close-up of the square in (c).

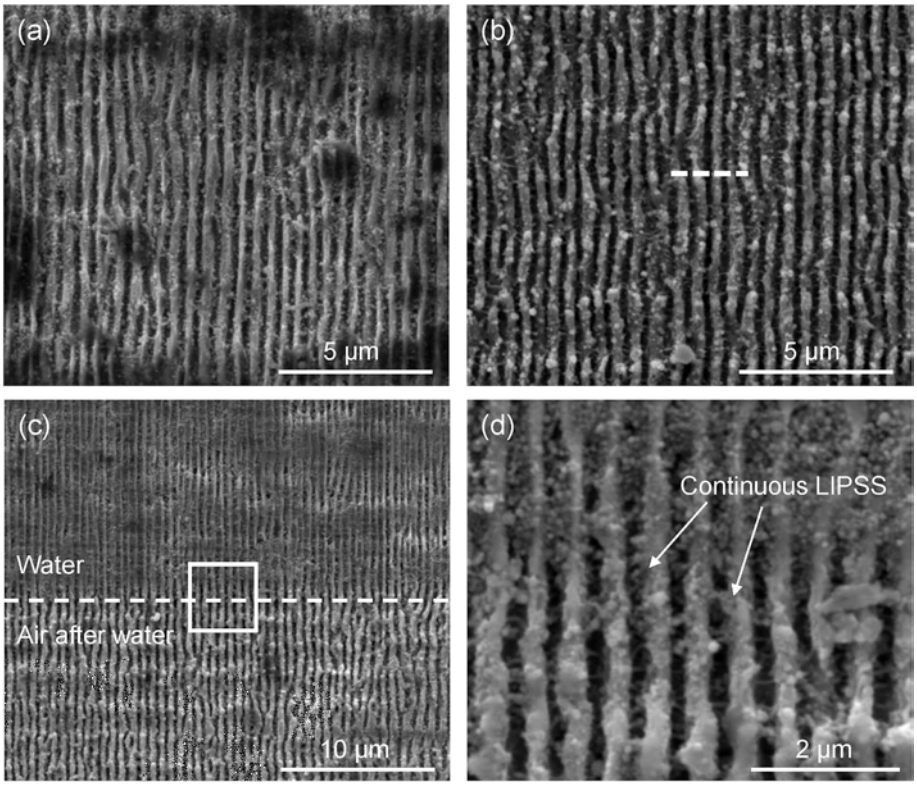

Fig. 10. SEM images of the surface (a) after first irradiation in water and (b) after second irradiation in the air; (c) boundary of (a) and (b); (d) close-up of the square in (c).

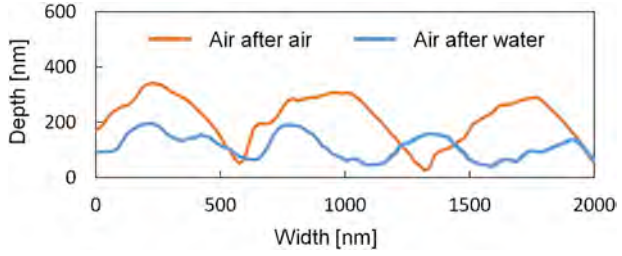

Fig. 11. Cross-sectional profiles of LIPSS in Figs. 9 (b) and 10 (b), showing different periods.

relaxation as a results of material self-organization, as shown in Fig. 13 (b). Laser irradiation causes emission of electrons, which makes the surface unstable [5,13]. As a result, LIPSS is assembled from the unstable surface through the perturbation effect. In this case, the near-surface layer of material will be reorganized and restructured during the laser pulse. Hence, even there are existing grooves or other structures on the surface, they will have little effect on the final LIPSS formation [5].

In this study, when the second laser irradiation was performed in the air, the resulting period of LIPSS was strongly dependent on the period of the previously formed LIPSS (Figs. 9 and 10). Therefore, LIPSS formation in the air is more likely due to the interference of incident laser and SPP. In contrast, the period of LIPSS formed by the second laser irradiation in water was distinctly different from the previously formed LIPSS (Fig. 12). From this result, it might be presumable that self-organization is the dominant mechanism for LIPSS formation in water. Due to the thermal effect caused by the suppressed plasma inside a liquid (Fig. 8), the unstable state of surface material facilitates lattice perturbation, and LIPSS is reassembled by surface restructuring.

To summarize, this study has demonstrated that the LIPSS formation mechanism of steels not only depends on material properties and laser parameters, but also strongly depends on the surrounding environments. It is possible to control the period and morphology of the LIPSS by utilizing the differences in the refractive index and thermal conductivity of various types of media. This might be technologically useful for surface functionalization of steel materials and provide added-value for future mechanical and/or optical products.

4. Conclusions

Picosecond pulsed laser was irradiated on a stainless tool steel surface in different kinds of media. It was found that the period of laser-induced periodic surface structure (LIPSS) formed in liquids was shorter than that formed in the air, and a strong relationship was identified between the period of LIPSS and the refractive index of the liquids. LIPSS formation was also affected by the thermal property of the liquid; in a liquid with low thermal conductivity, a mesh structure was formed on the irradiated surface rather than nanoscale grooves. The phenomenon of LIPSS reassembly in the laser irradiation of a surface with existing LIPSS indicated that the interference of incident laser and surface plasmon polariton might be dominant for LIPSS formation in the air; whereas the self-organization of surface material was the major

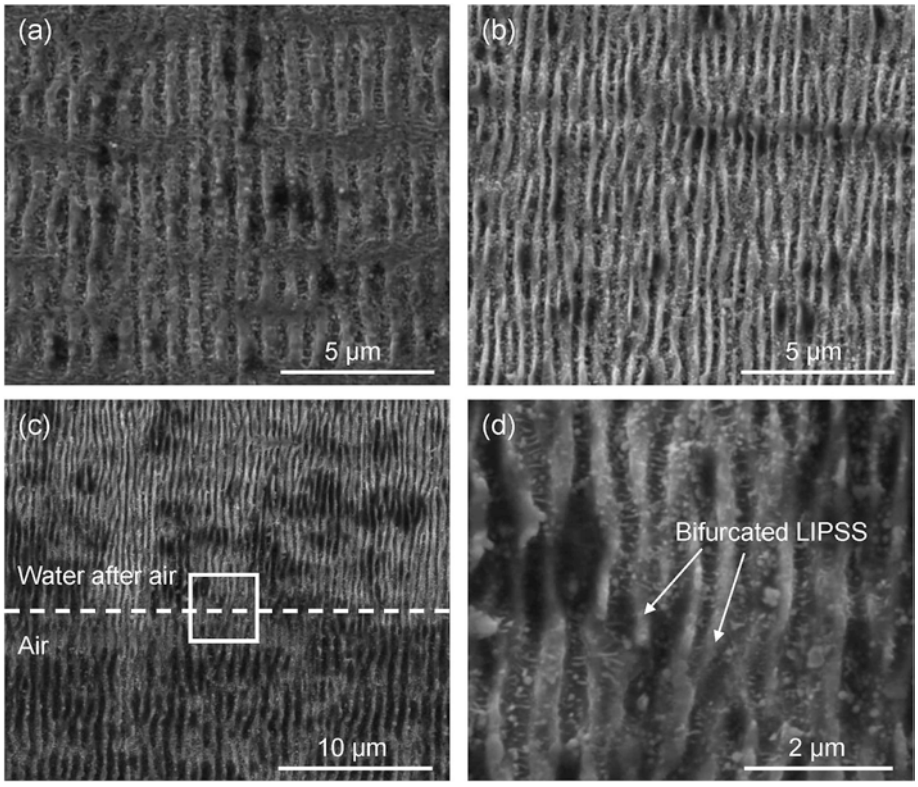

Fig. 12. SEM images of the surface (a) after first irradiation in the air, (b) after second irradiation in water; (c) boundary of (a) and (b); (d) close-up of the square in (c).

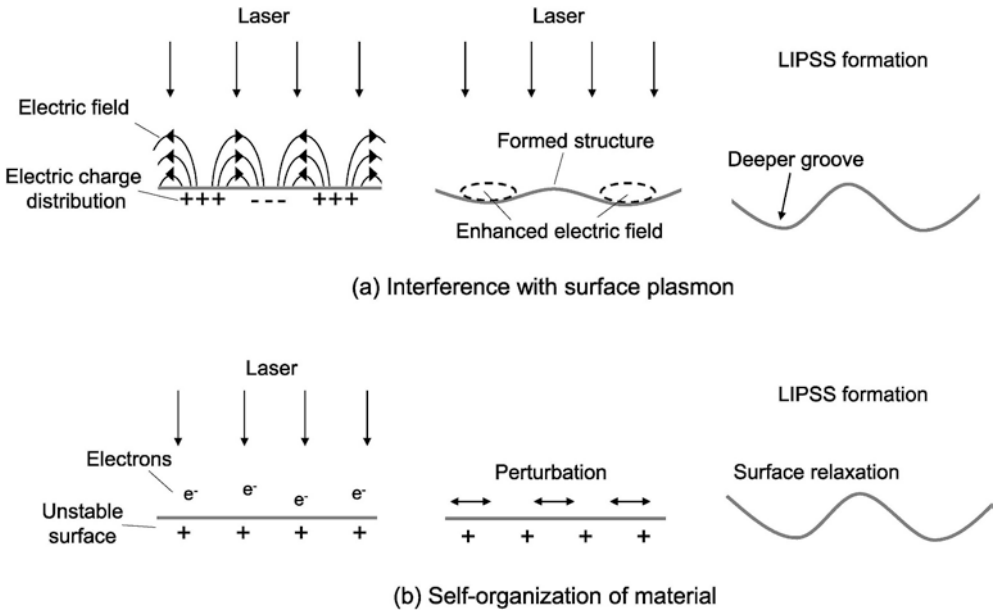

Fig. 13. Schematic of possible mechanisms of LIPSS formation: (a) interference of laser with surface plasmon, (b) self-organization of material surface.

mechanism for LIPSS formation in liquids. The findings from this study demonstrated the possibility of controlling the period and topography of LIPSS by using various media.

References

[1] Vorobyev AY, Makin VS, Guo C. Periodic ordering of random surface nanostructures induced by femtosecond laser pulses on metals. J Appl Phys 2007;101:034903.
[2] Bonse J, Krüger J, Höhm S, Rosenfeld A. Femtosecond laser-induced periodic surface structures. J Laser Appl 2012;24:042006.
[3] Tomita T, Kinoshita K, Matsuo S, Hashimoto S. Effect of surface roughening on femtosecond laser-induced ripple structures. Appl Phys Lett 2007;90:153115.
[4] Kobayashi T, Sera H, Wakabayashi T, Endo H, Takushima Y, Yan J. Surface flattening and nanostructuring of steel by picosecond pulsed laser irradiation. Nanomanuf Metrol 2018;1:1–8.
[5] Gregorčič P, Sedlaček M, Podgornik B, Reif J. Formation of laser-induced periodic surface structures (LIPSS) on tool steel by multiple picosecond laser pulses of different polarizations. Appl Surf Sci 2016;387:698–706.
[6] Vorobyev AY, Guo C. Femtosecond laser structuring of titanium implants. Appl Surf Sci 2007;253:7272–80.
[7] Borowiec A, Haugen HK. Subwavelength ripple formation on the surfaces of compound semiconductors irradiated with femtosecond laser pulses. Appl Phys Lett

2003;82:4462.
[8] Reif J, Varlamova O, Costache F. Femtosecond laser induced nanostructure formation self-organization control parameters. Appl Phys A 2008;92:1019–24.
[9] Wagner R, Gottmann J, Horn A, Kreutz EW. Subwavelength ripple formation induced by tightly focused femtosecond laser radiation. Appl Surf Sci 2006;252:8576–9.
[10] Vorobyev AY, Guo C. Effects of nanostructure-covered femtosecond laser-induced periodic surface structures on optical absorptance of metals. Appl Phys A 2007;86:321–4.
[11] Sakabe S, Hashida M, Tokita S, Namba S, Okamura K. Mechanism for self-formation of periodic grating structures on a metal surface by a femtosecond lase pulse. Phys Rev B 2009;79:033409.
[12] Bonse J, Rosenfeld A, Krüger J. On the role of surface plasmon polaritons in the formation of laser-induced periodic surface structures upon irradiation of silicon by femtosecond-laser pulses. J Appl Phys 2009;106:104910.
[13] Varlamova O, Costache F, Reif J, Bestehorn M. Self-organized pattern formation upon femtosecond laser ablation by circularly polarized light. Appl Surf Sci 2006;252:4702–6.
[14] Zhang Y, Zou G, Liu L, Zhao Y, Liang Q, Wu A, Zhou YN. Time-dependent wettability of nano-patterned surfaces fabricated by femtosecond laser with high efficiency. Appl Surf Sci 2016;389:554–9.
[15] Calderon MM, Rodríguez A, Ponte AD, Miñana MCM, Aranzadi MG, Olaizola SM. Femtosecond laser fabrication of highly hydrophobic stainless steel surface with hierarchical structures fabricated by combining ordered microstructures and LIPSS. Appl Surf Sci 2016;374:81–9.
[16] Wu B, Zhou M, Li J, Ye X, Li G, Cai L. Superhydrophobic surfaces fabricated by microstructuring of stainless steel using femtosecond laser. Appl Surf Sci 2009;256:61–6.
[17] Bonse J, Koter R, Hartelt M, Spaltmanm D, Pentzien S, Höhm S, Rosenfeld A, Krüger J. Femtosecond laser-induced periodic surface structures on steel and titanium alloy for tribological applications. Appl Phys A 2014;117:103–10.
[18] Vorobyev AY, Guo C. Colorizing metals with femtosecond laser pulses. Appl Phys Lett 2008;92:041914.
[19] Yao J, Zhang C, Liu H, Dai Q, Wu L, Lan S, Gopal AV, Trofimov VA, Lysak TM. Selective appearance of several laser-induced periodic surface structure patterns on a metal surface using structural colors produced by femtosecond laser pulses. Appl Surf Sci 2012;258:7625–32.
[20] Vorobyev AY, Guo C. Femtosecond laser-induced periodic surface structure formation on tungsten. J Appl Phys 2008;104:063523.
[21] Bonse J, Krüger J. Pulse number dependence of laser-induced periodic surface structures for femtosecond laser irradiation of silicon. J Appl Phys 2010;108:034903.
[22] Bonse J, Höhm S, Rosenfeld A, Krüger J. Sub-100-nm laser-induced periodic surface structures upon irradiation of titanium by Ti sapphire femtosecond laser pulses in air. Appl Phys A 2013;110:547–51.
[23] Qi L, Nihii K, Namba Y. Regular subwavelength surface structures induced by femtosecond laser pulses on stainless steel. Opt Lett 2009;34:12.
[24] Hwang TY, Guo C. Angular effects of nanostructure-covered femtosecond laser induced periodic surface structures on metals. J Appl Phys 2010;108:073523.
[25] Dufft D, Rosenfeld A, Das SK, Grunwald R, Bonse J. Femtosecond laser-induced periodic surface structures revisited: a comparative study on ZnO. J Appl Phys 2009;105:034908.
[26] Bashir S, Rafique MS, Nathala CS, Ajami AA, Husinsky W. Femtosecond laser fluence based nanostructuring of W and Mo in ethanol. Physica B 2017;513:48–57.
[27] Yao JW, Zhang CY, Liu HY, Dai QF, Wu LJ, Lan S, Gopal AV, Trofimov VA, Lysak TM. High spatial frequency periodic structures induced on metal surface by femtosecond laser pulses. Optic Express 2012;20:905–11.
[28] Shaheen ME, Gagnon JE, Fryer BJ. Laser ablation of iron: a comparison between femtosecond and picosecond laser pulses. J Appl Phys 2013;114:083110.
[29] Isselinm JC, Alloncle AP, Autric M. On laser induced single bubble near a solid boundary: contribution to the understanding of erosion phenomena. J Appl Phys 1998;84:5766.
[30] Yasaki R, Uchida H. Experiments on effective microbubble generation using a fine pores system. J Adv Sci 2008;20:24.
[31] Caizhen Y, Yayun Y, Baoshen J, Yuan L, Renjie D, Yong J, Yuxin W, Xiaodong Y. Polarization and fluence effects in femtosecond laser induced micro nano structures on stainless steel with antireflection property. Appl Surf Sci 2017;425:1118–24.
[32] Berthe L, Fabbro R, Peyre P, Tollier L, Bartnicki E. Shock waves from a water-confined laser-generated plasma. J Appl Phys 1997;82:2826.